Modulation of Seasonal Precipitation over the Tropical Western/Central Pacific by Convectively Coupled Mixed Rossby–Gravity Waves

TAKESHI HORINOUCHI

Faculty of Environmental Earth Science, Hokkaido University, Sapporo, Japan

(Manuscript received 15 October 2012, in final form 19 November 2012)

ABSTRACT

The relationship between the interannual variations of the activity of convectively coupled equatorial waves and seasonal mean precipitation in the tropical western to central Pacific Ocean is investigated. It is found that the convectively coupled mixed Rossby–gravity (MRG) waves are highly and negatively correlated with the seasonal precipitation near the equator in boreal summer. It is suggested that the MRG waves, which have convection centers off the equator, suppress the equatorial precipitation. The relation is insignificant in the other seasons, when the interannual variation of sea surface temperature near the equator is greater than in boreal summer. Also, a similar relation is not found in the eastern Pacific in any season.

1. Introduction

Since their theoretical (Matsuno 1966) and observational (Yanai and Maruyama 1966) findings, equatorially trapped wave modes have been studied extensively. Convectively coupled equatorial waves (CCEWs) are the equatorial waves in which moist convection is incorporated (e.g., Liebmann and Hendon 1990; Takayabu 1994; Wheeler and Kiladis 1999). The CCEWs typically have the equivalent depths h ranging from 10 to 50 m, whose smallness indicates a dynamical coupling with convection.

The CCEWs play important roles in the tropical troposphere [a review is made by Kiladis et al. (2009)]. They are known to interact with various atmospheric phenomena such as intraseasonal oscillations (e.g., Dunkerton and Crum 1995; Roundy and Frank 2004b), tropical cyclones (e.g., Bessafi and Wheeler 2006; Frank and Roundy 2006), and monsoon (e.g., Straub et al. 2006). Wang and Fu (2007) suggested that Amazon rainfall modulates the Atlantic ITCZ through Kelvin waves on a time scale of 10 days.

However, impacts of CCEWs on seasonal mean quantities are not known. This study is the first to report one. Here, the relationship among the interannual variations in seasonal mean precipitation, outgoing longwave radiation (OLR), SST, and CCEW activity is investigated. A focus is made on the convectively coupled mixed Rossby–gravity (MRG) waves, which are active over the western to central Pacific Ocean (Hendon and Liebmann 1991).

This study is motivated by the study by Horinouchi (2012). He studied the Hadley circulation and tropical precipitation by using a simplified AGCM with an "aquaplanet" configuration. In his study, changing the value of a tunable parameter of cumulus parameterization changed the Hadley circulation strength and the lateral distribution of tropical precipitation. The impact is substantial when SST is globally uniform, but it also exists when pole-to-equator SST gradients are present. This feature is associated with the activity of the CCEWs generated spontaneously in the model. Moreover, the lateral distribution of precipitation near the equator is associated with the dominant modes of CCEWs, which are somehow changed by changing the parameter. The result indicates an interaction between CCEWs and equatorial precipitation in the model.

This study is conducted to investigate whether a similar interplay exists in the real atmosphere. The distribution of tropical precipitation is known to be affected by fine meridional structures in SST near the equator (e.g., Lindzen and Nigam 1987; Back and Bretherton 2009). A focus is thus made on the tropical western to central Pacific in boreal summer, when SST is relatively smooth.

Corresponding author address: Takeshi Horinouchi, Faculty of Environmental Earth Science, Hokkaido University, N10W5 Sapporo, Hokkaido 060-0810, Japan.
E-mail: horinout@ees.hokudai.ac.jp

DOI: 10.1175/JAS-D-12-0283.1

TABLE 1. Parameters used to derive the amplitude of CCEWs. The second column shows the meridional preprocessing to obtain the symmetric (denoted as sym) or antisymmetric (anti) components. The third column specifies the spectral window for two-dimensional Fourier filtering, where k is zonal wavenumber (positive/negative for eastward/westward propagation, respectively), T is period (1/frequency), and c is the zonal phase velocity at the equator. The fourth column shows the latitudinal bands to average the rms meridionally to derive the representative amplitude.

Name	y filter	Spectral window	Latitudinal band
MRG1	anti	$k = -8$ to 0, $T = 3$ to 7 days	$\lvert\phi\rvert = 5°$ to 10°
MRG2	anti	$k = -8$ to -4, $T = 4$ to 7 days and $k = -3$ to 0, $T = 3$ to 7 days	$\lvert\phi\rvert = 5°$ to 10°
TD	none	$k = -15$ to -7, $T = 2$ to 5 days	5° to 10°N
KelvinMJO	sym	$k = 1$ to 8, $c = 3$ to 23 m s^{-1}	$\lvert\phi\rvert \le 7.5°$
Kelvin0	sym	$k = 1$ to 8, $c = 11$ to 23 m s^{-1}	$\lvert\phi\rvert \le 7.5°$

The rest of the paper is organized as follows. The data and analysis methods are presented in section 2. The results are presented in section 3, and conclusions are drawn in section 4.

2. Data and methodology

Data over 30 yr since 1982 are used in this study. Statistical analyses are made by using the 30 periods for each or one of the 3-month seasons: March–May (MAM), June–August (JJA), September–November (SON), and December–February (DJF). The datasets used are as follows: the daily and monthly mean National Oceanic and Atmospheric Administration (NOAA) interpolated OLR (Liebmann and Smith 1996), the monthly mean Global Precipitation Climatology Project (GPCP), version 2.2, precipitation (Adler et al. 2003), the monthly mean NOAA optimum interpolation SST version 2, and the monthly mean National Centers for Environmental Prediction (NCEP)/Department of Energy (DOE) Reanalysis 2. The horizontal resolutions of the SST and the other datasets are 1° and 2.5°, respectively.

Table 1 shows the parameters used to derive CCEW amplitudes. An rms amplitude is defined for each 90-day period from daily OLR as follows. After extracting meridionally symmetric or antisymmetric components with respect to the equator, the OLR is filtered spectrally with longitude and time. It is then squared and averaged over a limited longitudinal range of interest (specified in what follows) and the period. The CCEW amplitude is defined as its square root. For correlation analyses, it is further averaged over a latitudinal band in Table 1 to derive a representative amplitude, which is expressed as x regardless of wave type.

Background zonal wind is considered to define the spectral windows. Figure 1 shows the climatological zonal wind of JJA obtained by averaging over 130°E–170°W, 1000–400 hPa, and the 30 yr. Also shown are the mean wind plus/minus the standard deviation, which is obtained from the JJA mean zonal wind for each longitude, pressure level, and year; the standard deviation thereby does not include intraseasonal variability. From the result, the background zonal wind is considered as varying from 0 to -8 m s^{-1}.

Figure 2 shows the dispersion relation of MRG waves for $h = 12$ and 50 m, varying the background wind at the equator u_0. Also shown are the spectral windows used to extract convectively coupled MRG waves. The MRG1 filtering is mainly used in this study, although the spectral window of MRG2 is rather closer to the conventional window for convectively coupled MRG waves in which $u_0 = 0$ is assumed (e.g., Wheeler and Kiladis 1999). Note that the wave periods obtained from daily time series are limited to integer $(2, 3, 4, \ldots)$ days, so the differences are subtle. The TD filtering is introduced after Roundy and Frank (2004a) to pass signals from tropical depressions (TDs).

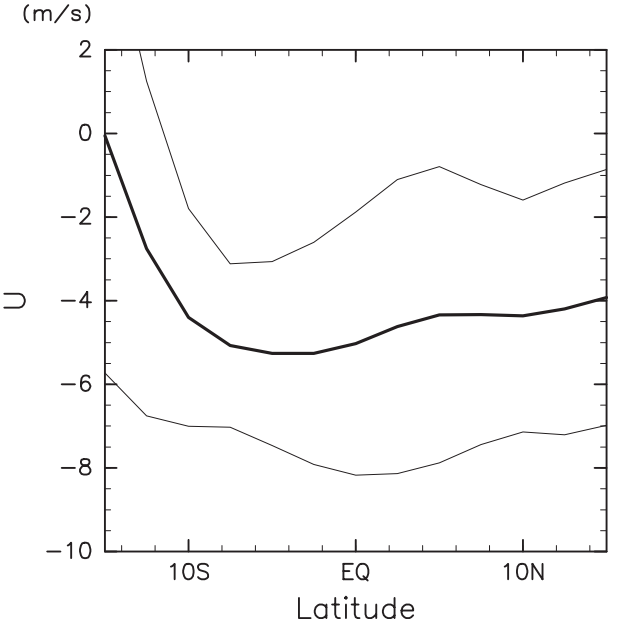

FIG. 1. Thick line: climatological zonal wind velocity of the JJA season obtained by averaging over 130°E–170°W, 1000–400 hPa, and the 30 yr. Thin lines: the climatological wind plus/minus the standard deviation of seasonal mean zonal winds (see the text).

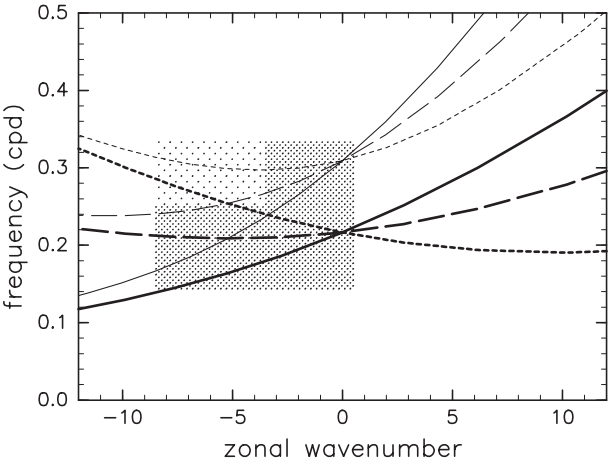

FIG. 2. Dispersion relation of the MRG waves (including the $n = 0$ eastward-propagating inertia–gravity modes) with $h = 12$ (thick lines) and 50 m (thin lines) for $u_0 = 0$ (solid), -4 (dashed), and -8 m s^{-1} (dotted). The darker shading shows the spectral window for the MRG2 filter, and the darker and lighter shadings, together, show the spectral window for the MRG1 filter.

Kelvin waves have intrinsic zonal phase velocities 10.8 and 22.1 m s^{-1} for $h = 12$ and 50 m, respectively. Considering $u_0 = -8$–0 m s^{-1}, the KelvinMJO filtering is defined to pass ground-based zonal phase velocities $c = 3$–23 m s^{-1}, which covers MJO signals too. The Kelvin0 filtering is also used to pass $c = 11$–23 m s^{-1} as the conventional Kelvin wave filtering assuming $u_0 = 0$.

The following quantities are introduced as the averages over a longitudinal range of interest, a specified latitudinal band, and a 3-month period for each year:

- s: SST over $\phi = 5°$S–5°N
- P: precipitation over $\phi = 2.5°$S–2.5°N
- R: OLR over $\phi = 2.5°$S–2.5°N

The correlation coefficient between quantities a and b is written as r_{ab}. The partial correlation between a and b excluding the effect of c is

$$r_{ab.c} = \frac{r_{ab} - r_{ac}r_{bc}}{\sqrt{1 - r_{ac}^2}\sqrt{1 - r_{bc}^2}}. \quad (1)$$

3. Results

a. Western to central Pacific in boreal summer

Results for the western to central Pacific (130°E–170°W) in boreal summer are shown in this subsection. Figures 3a–c shows the meridional distributions of mean SST, precipitation, and OLR for the JJA period for each year. The line colors show the values of SST s near the equator. The interannual variation of SST near the equator is about 1 K, which is smaller than in the other seasons shown later. The color distribution in Figs. 3b,c is irregular, and the overall correlation between s and precipitation (or OLR) is weak.

Figure 3d shows the meridional distributions of the MRG amplitudes obtained from the daily OLR by using the MRG1 filter. In Figs. 3e,f, mean precipitation and OLR are colored according to x, the MRG amplitude over $|\phi| = 5°$–10°. The correlation between x and the mean precipitation (or OLR) is high near the equator.

Correlations among seasonal indices over the 30 yr are shown in Figs. 3g–i and Table 2. The correlation between the MRG amplitude x and the precipitation P over 2.5°S–2.5°N is -0.75. Its significance is greater than 99.999% according to Student's t test. The correlation between x and R, the equatorial OLR, is 0.72, which is also significant on the same level. Therefore, the interannual variation of precipitation near the equator is highly correlated with the activity of convectively coupled MRG waves measured with OLR. Figures 3e,f show that the high correlation extends from 4° to 6°S. The equatorial precipitation is suppressed as the MRG amplitude is increased. On the other hand, the equatorial s has no significant correlation with x, P, or R.

The high correlation between the MRG amplitude and the equatorial precipitation is insensitive to the spectral window employed. The correlation coefficient between P and the MRG amplitude defined using MRG2 is -0.74, which is very close to the one using MRG1. Therefore, only MRG1 is used to define the MRG amplitude in what follows.

The sensitivity of r_{xP} to the longitudinal range is examined. Shifting it eastward by 10° or 20° does not affect the correlation much ($-r_{xP}$ exceeding 0.7), while shifting it westward deteriorates the correlation ($r_{xP} = -0.69$ for 120°E–180° and $r_{xP} = -0.38$ for 110°–170°E).

The correlations between x and the precipitation over other latitudinal bands (but again for longitudes 130°E–170°W) are as follows: -0.38 and 0.22 against precipitation over 5°–10°N and 5°–10°S, respectively. Note that these latitudinal bands are used to derive x. Therefore, these weak correlations indicate that the interannual variability of MRG waves measured in terms of OLR is not associated with the interannual variability of the off-equatorial mean precipitation.

The MRG1 and MRG2 spectral windows have some overlap with the spectral ranges attributed conventionally to TDs. In reality, transitions between MRGs and TDs have been observed (Kiladis et al. 2009). Thus, the TD filtering is used to examine which of the MRGs and TDs are relevant to the interannual variation of

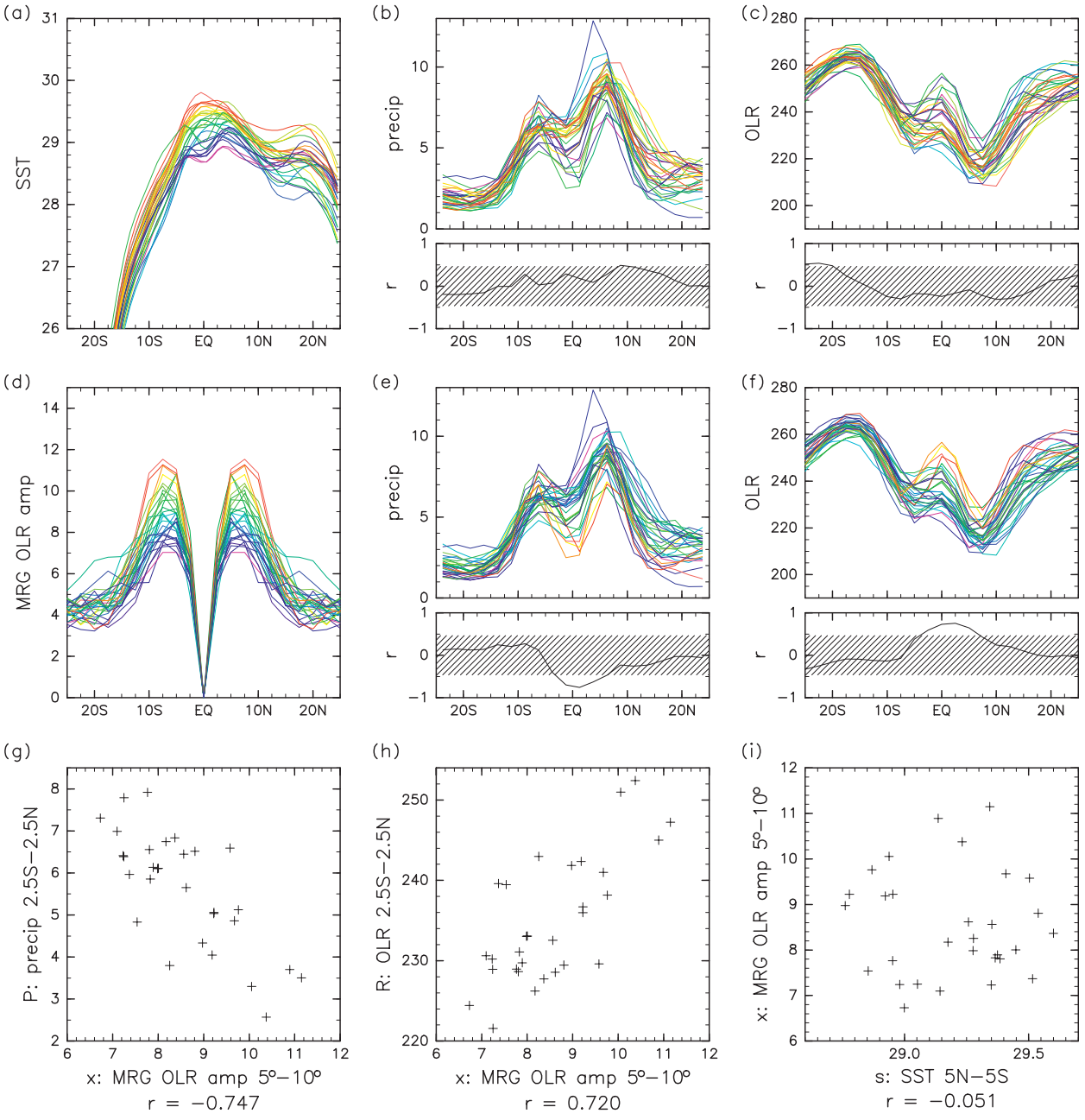

FIG. 3. Thirty-year statistics for the western to central Pacific (130°E–170°W) in boreal summer (JJA). (a) Meridional distributions of mean SST (°C) for the 30 JJA periods, colored according to its equatorial mean s; (b) (top) as in (a), but for mean precipitation (mm day^{-1}), also colored according to s, and (bottom) the correlation coefficient between the mean precipitation (for each latitude) and s, where hatching is made where the statistical significance is below 99%; (c) as in (b), but for OLR (W m^{-2}); (d) MRG amplitude obtained by using the MRG1 filter, colored according to its 5°–10° mean x; (e),(f) as in (b) and (c), respectively, but using x instead of s; (g) scatter diagram between x and the precipitation near the equator P, with the correlation coefficient shown below the panel; (h) as in (g), but for x and the OLR near the equator R; (i) as in (g), but for s and x.

equatorial precipitation. The result using the TD filer is $r_{xP} = -0.25$, indicating that TDs are unimportant.

One can speculate that precipitation near the equator may be more correlated with the activity of Kelvin waves than that of MRGs. When the KelvinMJO filter is used, r_{xP} is 0.48, which is significant by 99% but is weak (also, $r_{xP} = -0.32$ is insignificant). When the MJO signal is excluded by using the Kelvin0 filter, r_{xP} is −0.12, indicating no correlation. Therefore, the equatorial precipitation may have some positive correlation with the MJO, as

TABLE 2. Correlation and partial correlation coefficients among the 30 seasonal mean indices x, s, P, and R for each season over the western to central Pacific (130°E–170°W). The 30-yr climatology and the interannual standard deviation of x are also shown as $\langle x \rangle$ and σ_x (W m^{-2}), respectively. Correlations regarding s are omitted for brevity for filtering other than MRG1.

Filter	Season	$\langle x \rangle$	σ_x	r_{xP}	r_{xR}	r_{sP}	r_{sR}	r_{xs}	$r_{xP.s}$	$r_{xR.s}$
MRG1	JJA	8.55	1.16	−0.75	0.72	0.23	−0.21	−0.05	−0.76	0.73
TD	JJA	10.5	1.05	−0.25	0.23					
KelvinMJO	JJA	12.2	1.57	0.48	−0.32					
Kelvin0	JJA	7.53	0.86	−0.12	0.08					
MRG1	SON	9.63	1.34	−0.46	0.43	0.63	−0.65	−0.18	−0.46	0.42
MRG1	DJF	7.39	0.83	−0.36	0.33	0.67	−0.68	0.03	−0.51	0.49
MRG1	MAM	7.57	0.97	−0.12	0.13	0.74	−0.70	−0.02	−0.15	0.17

one may expect, but it is not correlated with the convectively coupled Kelvin wave amplitude in boreal summer.

It has been shown that the amplitude of convectively coupled MRG waves is highly and negatively correlated with equatorial precipitation. Therefore, there may be some causal relationship between them. It is, however, not very conceivable that equatorial precipitation affects MRGs without much affecting Kelvin waves that have convergence/divergence centers around the equator. It is rather likely that the MRGs affect the equatorial precipitation. In convectively coupled MRG waves, convection centers are located off the equator. Thus, the MRGs may suppress the equatorial precipitation; for instance, the equatorial meridional winds associated with them may transport moisture to converge and precipitate off the equator. Further study would be needed to quantify the causality.

b. *Seasonal variation/brief note on the eastern Pacific*

Figure 4 shows seasonal mean SST, precipitation, and OLR over the western to central Pacific (130°E–170°W) as in Figs. 3a–c but for SON, DJF, and MAM. In these seasons, SST near the equator has larger interannual variations than in JJA. The equatorial minimum is deeper in some years than in JJA. As a result, equatorial precipitation and OLR are more correlated with SST (Table 2). In these seasons, $|r_{sP}|$ and $|r_{sR}|$ are greater than 0.6. Correlations r_{xP} and r_{xR} (x is the MRG1 amplitude throughout this subsection) have the same signs as in JJA, but they are weak. Also, r_{xs} is weak, so the partial correlation excluding the effect of the equatorial SST, $r_{xP.s}$, is similar to r_{xP}.

The reason why even the partial correlations are smaller in these seasons than in JJA is not clear. One can speculate that the dominance of the SST effect may decouple the MRGs and the equatorial mean precipitation. Or there might be other processes that affect the equatorial precipitation, especially in boreal fall when MRG is climatologically strong ($\langle x \rangle$ in Table 2); the peak in boreal summer or fall has been reported (Hendon and Liebmann 1991; Roundy and Frank 2004a; Yasunaga 2011).

Hendon and Liebmann (1991) hypothesized that convectively coupled MRG waves are favorably generated if SST is minimized at and symmetric with respect to the equator. However, the weak correlation between x and s indicates that the equatorial SST minimum is not crucial. Additional analyses are made to investigate the impact of the meridional symmetry of SST. Here, the absolute differences between SSTs averaged over 10°S–0° and 10°N–0°, termed z, is used. In JJA, r_{xz} is −0.54, which is consistent with the hypothesis (z decreases with symmetry). The partial correlation $r_{xP.z}$ is −0.65, which is weaker than r_{xP} and $r_{xP.s}$. However, it is still highly significant, so the strong r_{xP} is not the artifact of the correlation between x and z. Also, $r_{zP} = 0.52$ is weaker than r_{xP}. Several quantities on the symmetry have been tested, and the result is robust. In the other seasons, r_{xz} is insignificant.

The correlation analyses are also conducted for the eastern Pacific (170°–90°W). The interannual variations of equatorial precipitation and OLR are dominated by that of SST (not shown). There is no season in which the MRG activity may have a significant impact on the mean precipitation in the eastern tropical Pacific. Note that convectively coupled MRG waves are weak in the eastern Pacific (Kiladis et al. 2009).

4. Conclusions

The relationship among the interannual variations of CCEW amplitudes, seasonal mean precipitation, OLR, and SST near the equator has been investigated. In the western to central Pacific in boreal summer, the amplitude of the convectively coupled MRG waves is highly correlated with precipitation near the equator, where the precipitation is suppressed as the MRG amplitude is increased. It is suggested that the convectively coupled MRG waves, which have convection centers off the equator, suppress the equatorial precipitation. The

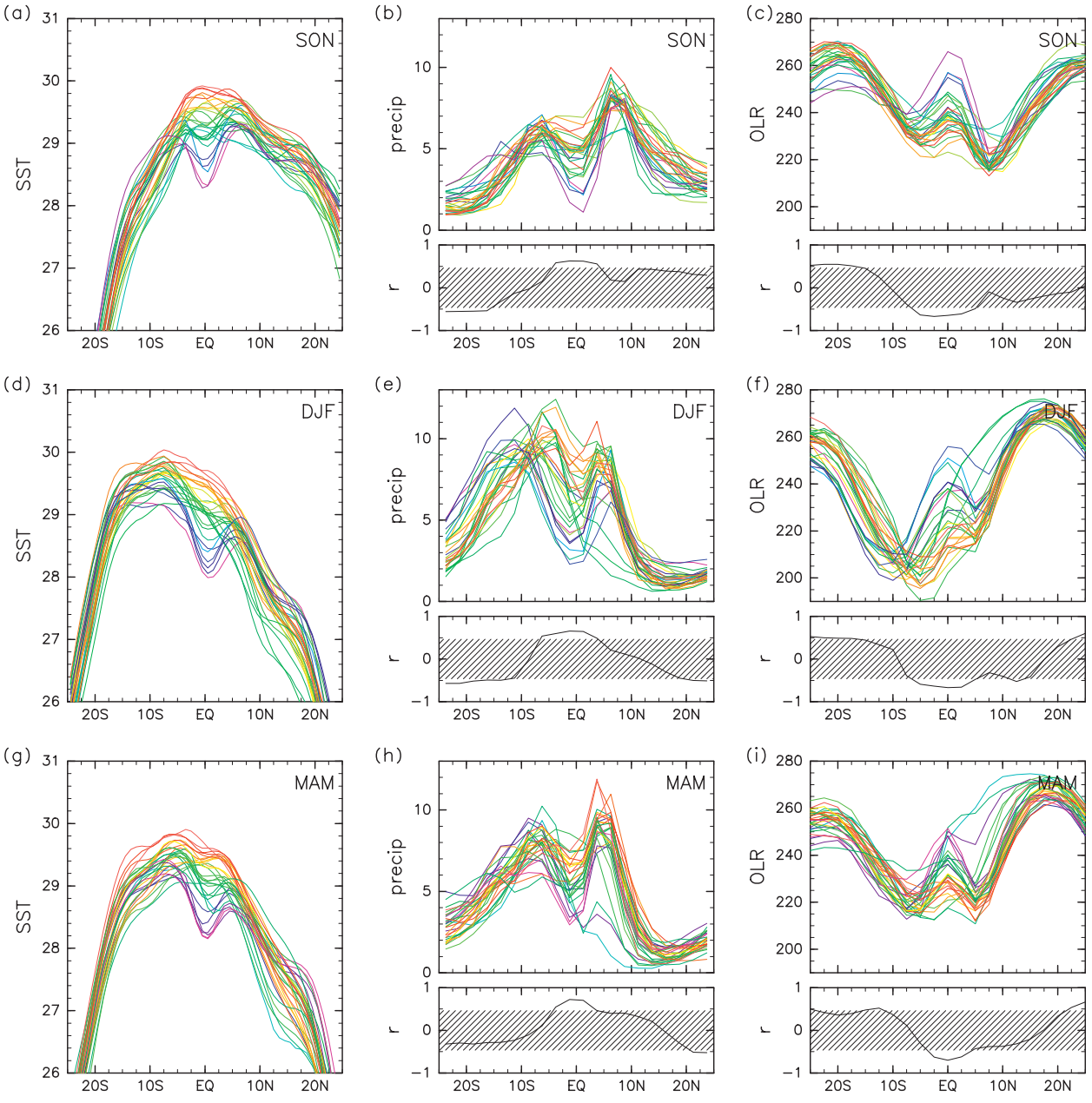

FIG. 4. As in Figs. 3a–c, but for the other seasons: (a)–(c) SON, (d)–(f) DJF, and (g)–(i) MAM.

equatorial precipitation has a weak positive correlation with the combined Kelvin wave–MJO amplitude, but it has little correlation with the convectively coupled Kelvin wave amplitude assuming $u_0 = 0$.

The relationship between the MRG amplitude and the equatorial precipitation is highly significant only in boreal summer. In the other seasons, the interannual variation of precipitation near the equator is dominated by that of SST. Also, in the eastern Pacific, the MRG amplitude is not correlated with the equatorial precipitation in any season.

The factor that controls the seasonal mean activity of CCEWs has not been elucidated in this study. Also, the impacts of CCEWs on the precipitation over the regions other than the Pacific are yet to be studied.

Acknowledgments. The author thanks two anonymous reviewers for helpful comments. This study is supported in part by the JSPS Grant 22540444. The data used are provided by the NOAA/OAR/ESRL PSD, Boulder, Colorado, from their website at http://www.esrl.noaa.gov/psd/.

REFERENCES

Adler, R. F., and Coauthors, 2003: The Version-2 Global Precipitation Climatology Project (GPCP) Monthly Precipitation Analysis (1979–present). *J. Hydrometeor.,* **4,** 1147–1167.

Back, L. E., and C. S. Bretherton, 2009: On the relationship between SST gradients, boundary layer winds, and convergence over the tropical oceans. *J. Climate,* **22,** 4182–4196.

Bessafi, M., and M. C. Wheeler, 2006: Modulation of south Indian Ocean tropical cyclones by the Madden–Julian oscillation and convectively coupled equatorial waves. *Mon. Wea. Rev.,* **134,** 638–656.

Dunkerton, T. J., and F. X. Crum, 1995: Eastward propagating ~2- to 15-day equatorial convection and its relation to the tropical intraseasonal oscillation. *J. Geophys. Res.,* **100** (D12), 25 781–25 790.

Frank, W. M., and P. E. Roundy, 2006: The role of tropical waves in tropical cyclogenesis. *Mon. Wea. Rev.,* **134,** 2397–2417.

Hendon, H. H., and B. Liebmann, 1991: The structure and annual variation of antisymmetric fluctuations of tropical convection and their association with Rossby–gravity waves. *J. Atmos. Sci.,* **48,** 2127–2140.

Horinouchi, T., 2012: Moist Hadley circulation: Possible role of wave–convection coupling in aquaplanet experiments. *J. Atmos. Sci.,* **69,** 891–907.

Kiladis, G. N., M. C. Wheeler, P. T. Haertel, K. H. Straub, and P. E. Roundy, 2009: Convectively coupled equatorial waves. *Rev. Geophys.,* **47,** RG2003, doi:10.1029/2008RG000266.

Liebmann, B., and H. H. Hendon, 1990: Synoptic-scale disturbances near the equator. *J. Atmos. Sci.,* **47,** 1463–1479.

——, and C. A. Smith, 1996: Description of a complete (interpolated) outgoing longwave radiation dataset. *Bull. Amer. Meteor. Soc.,* **77,** 1275–1277.

Lindzen, R. S., and S. Nigam, 1987: On the role of the sea surface temperature gradients in forcing the low-level winds and convergence in the tropics. *J. Atmos. Sci.,* **44,** 2418–2436.

Matsuno, T., 1966: Quasi-geostrophic motions in the equatorial area. *J. Meteor. Soc. Japan,* **44,** 25–43.

Roundy, P. E., and W. M. Frank, 2004a: A climatology of waves in the equatorial region. *J. Atmos. Sci.,* **61,** 2105–2132.

——, and ——, 2004b: Effects of low-frequency wave interactions on intraseasonal oscillations. *J. Atmos. Sci.,* **61,** 3025–3040.

Straub, K. H., G. N. Kiladis, and P. E. Ciesielski, 2006: The role of equatorial waves in the onset of the South China Sea summer monsoon and the demise of El Niño during 1998. *Dyn. Atmos. Oceans,* **42,** 216–238.

Takayabu, Y. N., 1994: Large-scale cloud disturbances associated with equatorial waves. Part I: Spectral features of the cloud disturbances. *J. Meteor. Soc. Japan,* **72,** 433–448.

Wang, H., and R. Fu, 2007: The influence of Amazon rainfall on the Atlantic ITCZ through convectively coupled Kelvin waves. *J. Climate,* **20,** 1188–1201.

Wheeler, M., and G. N. Kiladis, 1999: Convectively coupled equatorial waves: Analysis of clouds and temperature in the wavenumber–frequency domain. *J. Atmos. Sci.,* **56,** 374–399.

Yanai, M., and T. Maruyama, 1966: Stratospheric wave disturbances propagating over the equatorial Pacific. *J. Meteor. Soc. Japan,* **44,** 291–294.

Yasunaga, K., 2011: Seasonality and regionality of the Madden-Julian oscillation and convectively coupled equatorial waves. *SOLA,* **7,** 153–156, doi:10.2151/sola.2011-039.